Advances in Environmental Technology 2 (2018) 95-105

Advances in Environmental Technology

journal homepage: http://aet.irost.ir

Preparation and characterization of MWCNT-COOH/PVC ultrafiltration membranes to use in water treatment

Sepideh Masoumi [a,b], Ali Reza Miroliaei[a,*], Yoones Jafarzadeh[b,c,*]

[a] *Department of Chemical Engineering, University of Mohaghegh Ardabili, Ardabil, Iran.*

[b] *Membrane Technology Research Center, Sahand University of Technology, Tabriz, Iran.*

[c] *Faculty of Chemical Engineering, Sahand University of Technology, Tabriz, Iran.*

ARTICLE INFO

Article history:
Received 12 June 2018
Received in revised form
18 September 2018
Accepted 18 September 2018

Keywords:
PVC
MWCNT
Membrane
Ultrafiltration
Humic acid

ABSTRACT

Polyvinyl chloride (PVC) membranes containing pristine and modified multiwall carbon nanotube (MWCNT) were prepared and characterized. MWCNT was modified in order to achieve well-dispersion within the membranes. The results of FTIR analysis revealed that MWCNT was successfully carboxylated. The FESEM images indicated that the number of pores on the surface of membranes increased at the presence of pristine and modified MWCNT and the pore size distribution curves shifted towards smaller pores. The hydrophilicity, pure water flux, tensile strength and abrasion resistance of the membranes increased with increasing the content of MWCNT and COOH-MWCNT up to 0.3 wt. % and then decreased due to the agglomeration of nanotubes. Nevertheless, at the same content of nanotubes, COOH-MWCNT had more effect than MWCNT. The performance of the membranes was studied by filtration of humic acid (HA) solution and the results showed that HA rejection reached a peak of 96.88% for 0.3 wt. % PVC/MWCNT-COOH nanocomposite membrane. Finally, it was found that the antifouling properties of the membranes increased with increasing nanotube content, especially COOH-MWCNT.

1. Introduction

During the last decades, water shortages and the increasing demand for water to meet household, agricultural and industrial needs have resulted in a greater interest in water and wastewater treatment technologies [1,2]. Recently, membrane separation technologies have gained an important place in water purification [3,4]. Nowadays, polymeric membranes are widely used in membrane separations processes because of their advantages which include good film forming ability, flexibility and low cost [5,6]. Polyvinyl chloride (PVC) is an outstanding membrane material due to its stiffness, excellent physical, thermal and chemical properties, high resistance to corrosion, acids and alkalis, robust mechanical strength, and low cost in comparison with the other polymers [7,8]. Despite these remarkable properties, its poor hydrophilic nature results in membrane fouling and hinders its application in water and wastewater treatment [9,10]. Blending it with hydrophilic materials [11,12] and hydrophilic polymers [10] are two of the many methods that have been used to modify the PVC membrane and enhance its hydrophilicity. Among these methods, blending it with hydrophilic materials has attracted much attention in recent years. Behboudi et al. [11] prepared PVC/TiO_2 nanocomposite membranes via the non-solvent induced phase separation (NIPS) method. The results showed that even though the hydrophilicity, pure water flux and antifouling properties of the nanocomposite membranes were higher than those of the neat PVC membrane, the rejection of the composite membranes was reduced due to the increase in mean pore radius. Rabiee et al. [12] modified PVC ultrafiltration membranes with the

*Corresponding author. Tel: +984533513922
E-mail address: armiroliaei@uma.ac.ir
*Corresponding author. Tel: +984133459161
E-mail address: yjafarzadeh@sut.ac.ir
DOI: 10.22104/AET.2018.2965.1144

addition of zinc oxide (ZnO) nanoparticles. The results showed that ZnO led to an increase in the water flux of the membranes, remarkable changes in the membranes' structure, higher connectivity among channels, and a more porous structure. In a recent study by Demirel et al., PVC membranes were modified by dispersing Fe_2O_3 nanoparticles into the casting solution [13] The filtration performance tests revealed that pure water flux and the rejection of the nanocomposite membranes were enhanced significantly with the addition of Fe_2O_3 in comparison with the PVC membrane; this was due to higher porosity and pore size as well as a more hydrophilic surface of the modified membranes. One emerging additive material which can improve the properties of polymeric membranes is carbon nanotube (CNT) [14,15]. CNTs are graphite sheets rolled into circular bundles with both single-walled (SW) and multi-walled (MW) versions. Recently, the multi-walled carbon nanotubes (MWCNTs) have attracted much attention in membrane technology and wastewater treatment due to their promising properties: excellent mechanical strength, high chemical stability, adsorption capability, high surface area and unique one-dimensional tubular structure that acts as extraordinary mass transport channel [14]. However, the agglomeration of MWCNTand their hydrophobic nature could be a barrier for their application in polymer membranes [16]. There are several techniques to improve the dispersion of MWCNT in polymer membranes such as in-situ polymerization and chemical fictionalizations [16]. To overcome their hydrophobic nature, MWCNT can easily be modified by different functional groups such as hydrogen [17], nitrenes [18], fluorine [19], carbenes [20], radicals [21] and aryl radicals [22]. Suhartono and Tizaoui [23] fabricated composite PVDF/CNTs membranes via the phase inversion technique and optimized the content of two pristine and oxidized CNTs. The study showed that *1-Methyl 2-pyrrolidone (NMP)* was an excellent dispersing solvent for both CNTs, although the presence of oxidized functional groups on the plasma oxidized CNTs gave a better affinity of the CNTs-O towards NMP. Given the significant enhancement in water permeation and the enhanced rejection of solutes in addition to improved mechanical properties, CNTs-O/PVDF membranes showed a great potential to develop a robust UF membrane technique for water purification. Daraei et al. [24] fabricated a PES nanofiltration membrane using polyacrylic acid modified MWCNT. The addition of various amounts of PAA-g-MWCNT resulted in membranes with a high water flux and salt rejection capability. Vatanpour and his co-workers [25] prepared PES membranes embedded with acid oxidized MWCNT, and the results revealed that the hydrophilicity and antifouling properties of the prepared membranes were enhanced due to the migration of functionalized MWCNT to the membrane surface.

To the best of our knowledge, there are no reports about PVC membranes embedded with neat and modified MWCNT. The aim of the present work is to study the impact of pristine and modified MWCNT on the structure and performance of the PVC membrane. MWCNT were modified by acid treatment methods, and the membranes were prepared via the NIPS method. After the characterization of the membranes, they were used in the removal of humic acid from water.

2. Materials and methods

2.1. Materials

The PVC (MW=90000) *was supplied by the Arvand Petrochemical Company, Iran. The MWCNT (95%, 10 µm length and 10–30 nm in outer diameter) were purchased from the Petroleum Research Center, Iran. The 1-Methyl 2-pyrrolidone (NMP) as the polymer solvent was purchased from the Daejung Chemical and Metal, Korea. The polyethylene glycol (PEG) with a molecular weight of 200 Da, humic acid,* HNO_3 (67%) and H_2SO_4 (98%) were purchased from Merck. The silicon carbide particles (42-47 *µm) were purchased from Sigma-Aldrich, USA.*

2.2. Functionalization of MWCNT

The pristine MWCNT were functionalized by oxidation in a concentrated acidic environment. For this purpose, 0.1 gr of MWCNT was added to 100 mL of the acidic mixture with a 1/3 volume of sulfuric acid (H_2SO_4) to nitric acid (HNO_3), and the mixture was placed in an ultrasonic bath for 3 hours at 40 °C. The mixture was then diluted with distilled water to reach neutral pH. To separate the solid particles (MWCNT-COOH) the mixture was centrifuged. The resulting product was washed with distilled water and ethanol. Then the product was dried at 60 °C for 12 h in a heating oven.

2.3. Preparation of *UF pure PVC and nanocomposite membranes*

The on-solvent induced phase separation (NIPS) method was applied to prepare the membranes.For each specific membrane, a certain amount of MWCNT and MWCNT-COOH were dispersed and sonicated in NMP for 1 h; then, PEG was added to the dispersion and stirred for about 30 min. Subsequently, a certain amount of PVC was added to the suspension and stirred for at least 24 h to obtain a homogenous solution. The solution was allowed to degas for 2 h and then casted on a glass plate using a casting knife (CoaTest, Taiwan) at room temperature. The plate was immediately immersed in distilled water, as the non-solvent, at 30 °C to induce phase separation until the formed membranes became freely detached from the plate. The water bath was refreshed three times to complete the solvent exchange. Finally, the membranes were dried and stored at 5◦C. *The conditions under which* the membranes were prepared are listed in Table 1.

Table 1. Composition of prepared nanocomposite membranes.

Membrane	Polymer and nanoparticles (17.5 wt. %)		Pore former (2.5 wt.%)	Solvent (82.5 wt.%)
	PVC	MWCNT or MWCNT-COOH	PEG	NMP
Neat PVC	17.5	0	2.5	82.5
PVC/MWCNT (0.1 wt. %)	17.4	0.1	2.5	82.5
PVC/MWCNT (0.3 wt. %)	17.2	0.3	2.5	82.5
PVC/MWCNT (0.5 wt. %)	17.0	0.5	2.5	82.5
PVC/MWCNT (0.7 wt. %)	16.8	0.7	2.5	82.5
PVC/MWCNT-COOH (0.1 wt. %)	17.4	0.1	2.5	82.5
PVC/MWCNT-COOH *(0.3 wt. %)*	17.2	0.3	2.5	82.5
PVC/MWCNT-COOH *(0.5 wt. %)*	17.0	0.5	2.5	82.5
PVC/MWCNT-COOH (0.7 wt. %)	16.8	0.7	2.5	82.5

2.4. Characterization of functionalized MWCNT and membranes

2.4.1. Static contact angle measurement

The hydrophilic/hydrophobic characteristics of the membranes were examined by measuring the contact angle between the membrane surface and water droplet using a contact angle goniometer (PGX, Thwing-Albert Instrument Co.). In order to minimize the inaccuracy of the measurement, at least 5 contact angles on different locations of the samples were measured and the average value was reported.

2.4.2. Fourier transform infrared (FTIR) spectroscopy

The Fourier Transformed Infrared (FT-IR) analysis was used to investigate any alteration in the chemical composition of functionalized MWCNT; it was also employed to study the chemical structure and the type of functional groups created on the membrane surface. The results were recorded using a TENSOR 27 spectrometer (Bruker, Germany) in the range of 600–4000 cm^{-1} and at room temperature. The sample pellet of nanoparticles for the FTIR analysis was prepared by mixing the particles with KBr.

2.4.3. Mechanical properties

The tensile strength and elongation-at-break of the membranes were measured using a tensile test machine (STM-5, SANTAM, Iran). The samples were cut into 5 cm × 1cm in length and width, respectively. The effective length was 3 cm and two edges by the length of 1cm were stuck in the machine and the thickness of each sample was measured by using a micrometer. Each membrane sample was stretched at an extension rate of 50 mm/min at room temperature. Three trials were conducted for each sample, and the mean values were reported.

2.4.4. Abrasion resistance test

To examine the abrasion resistance of the prepared membranes, an accelerated testing setup was designed that was similar to the method described by Lai et al. [26]. Briefly, samples of the membranes were secured and immersed in 10 wt. % silicon carbide slurry. The slurry was then stirred for at least 7 days to allow the membranes to be in contact with abrasive silicon carbide particles. The weight of the samples before and after the abrasion test were measured to determine weight loss due to the abrasion.

2.4.5. Field Emission-Scanning Electron Microscope (FE-SEM)

The surface and cross-section morphologies of the membranes were visualized by FESEM (FESEM; MIRA3 FEG-SEM, Tescan) operating at 15 kV.

2.4.6. Pore size distribution

The pore size distribution and pore density (the number of pores per unit area) were estimated by analyzing the surface FESEM images of the membranes using Image Analysis software.

2.4.7. Filtration test

A laboratory bench scale dead end system was used to study pure water flux (PWF) and filtration of the HA solution. The system consisted of a membrane filtration cell, feed reservoir (HA tank), a pressure gauge to show the equilibrium pressure, and a cup connected to an N_2 balloon to provide the driving force. After measuring the pure water flux (J_0), the membrane modulus was connected to the HA filtration system. The filtration experiment was performed for 240 min using 1 mg/L HA solution to simulate the organic matter in natural waters at ambient temperature (25◦C). After that, the modulus was again connected to the pure water tank and the pure water flux after fouling (J_1) was

measured. Then the cake layer on the membrane was gently removed mechanically by a sponge and the membrane was washed with deionized water. Finally, the membrane was held in the modulus and connected to the pure water permeation system and pure water flux after rinsing (J_2) was measured. The pure water flux (J) was determined by the direct measurement of the permeate volume over the permeation time at 2 bar using Eq. (1):

$$J = \frac{m}{A \rho t} \quad (1)$$

where J is pure water flux (PWF) (L/m^{2}h), A is membrane area (m^2), and t is the time (h). For unmodified and modified membranes, the pure water flux was measured three times and the average value was reported. The total fouling ratio (TFR) can be calculated by Eq. (2) [27]:

$$TFR = (\frac{J_1 - J_0}{J_1}) \times 100 \quad (2)$$

The reversible fouling ration (RFR) can be calculated by Eq. (3):

$$RFR = (\frac{J_2 - J_0}{J_1}) \times 100 \quad (3)$$

The irreversible fouling ratio (IFR) can be calculated by Eq. (4):

$$IFR = (\frac{J_1 - J_2}{J_1}) \times 100 \quad (4)$$

The flux recovery (FR) can be calculated by Eq. (5):

$$FR = (\frac{J_2}{J_1}) \times 100 \quad (5)$$

And from the above equations, it is obvious that:

$$TFR = RFR + IFR \quad (6)$$

2.4.8. Membranes rejection

To evaluate membrane performance, the rejection of the membranes was measured based on the concentrations of HA in the permeation, and the feed solutions (C_p and C_f) were determined by an UV-spectrophotometer. The rejection R (%) was defined as Eq. (7):

$$R = (1 - \frac{C_p}{C_f}) \times 100 \quad (7)$$

3. Results and discussion

3.1. Contact angle and FTIR analysis

The contact angle is an important parameter for measuring surface hydrophilicity [28]. The smaller contact angle leads to higher hydrophilicity [29]. The contact angle data of the neat PVC and nanocomposite membranes are shown in Figure 1. The results show that the contact angle for both types of nanocomposite membranes is lower than the neat PVC. In addition, compared to the membranes with MWCNT, the MWCNT-COOH membranes show the lower contact angle. Thus, it can be confirmed that the MWCNT-COOH membranes had the better hydrophilicity [30]. Chelik et al. reported that CNT spontaneously migrated to the membrane surface during the phase inversion process [31-33]. The highest hydrophilicity and minimum contact angle, reaching 70.02° in the PVC/MWCNT nanocomposite membranes, indicated that the hydrophilicity of the membranes increased as a result of modification with the MWCNT. This improvement in PVC/MWCNT-COOH could also be explained by hydrophilic COOH groups present on the surface of the modified MWCNT. Figure 2 shows the FTIR spectra of three membranes (PVC, PVC/MWCNT and PVC/MWCNT-COOH) as well as the neat and modified MWCNT. For the PVC/MWCNT-COOH membrane, the peaks at 3400 and 1620 cm^{-1} were attributed to OH stretching vibration due to the hydroxyl group in the modified MWCNT which confirmed the modification of the MWCNT and their presence in the PVC/MWCNT-COOH membrane. In addition, the surface porosity affected the contact angle. With an increase in the surface porosity, the water drop could gradually penetrate into the pores due to the capillary force and consequently, the contact angle decreased [34]. In general, increasing the hydrophilicity of the membrane improved fouling resistance as well as water permeability because the water adsorption of the hydrophilic membranes was higher than that of the hydrophobic ones [35]. However, when the content of the MWCNT and MWCNT-COOH reached 0.3 wt%, the contact angle value increased, due to the aggregation of nanoparticles reducing the effective surface of hydrophilic groups.

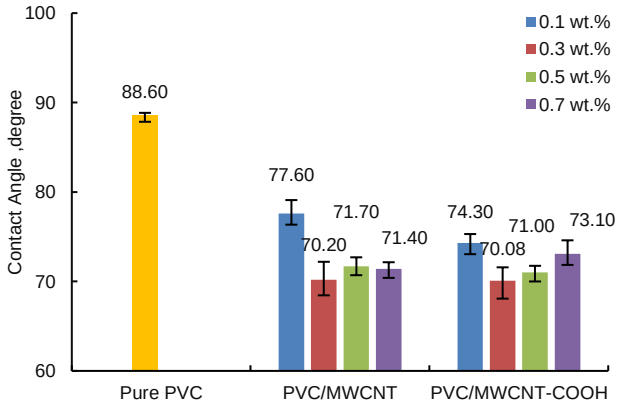

Fig. 1. Static water contact angle of the prepared membranes

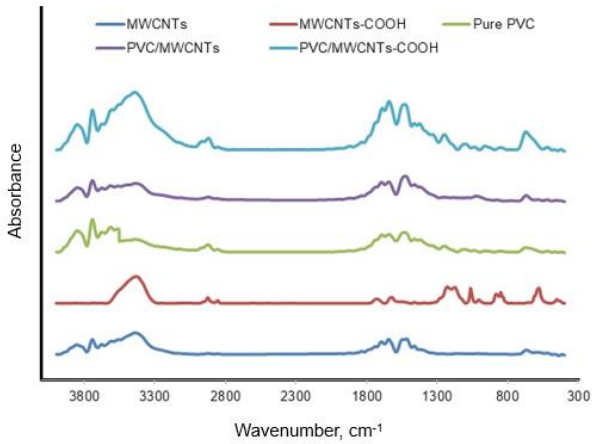

Fig. 2. FT-IR spectra of MWCNT and MWCNT-COOH nanoparticles and PVC, PVC/MWCNT and PVC/MWCNT-COOH membranes

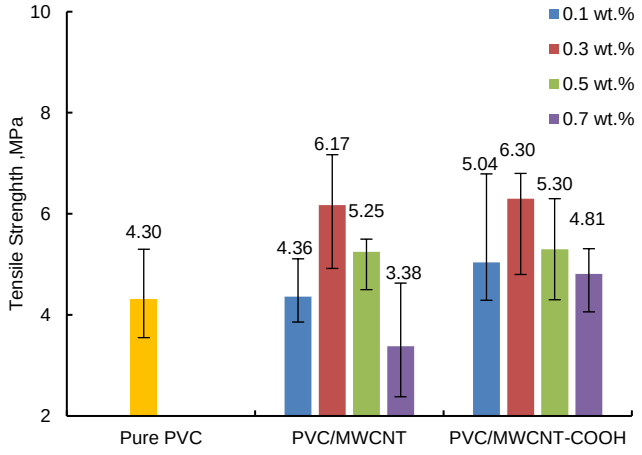

Fig. 3. Tensile strength content values for prepared membranes.

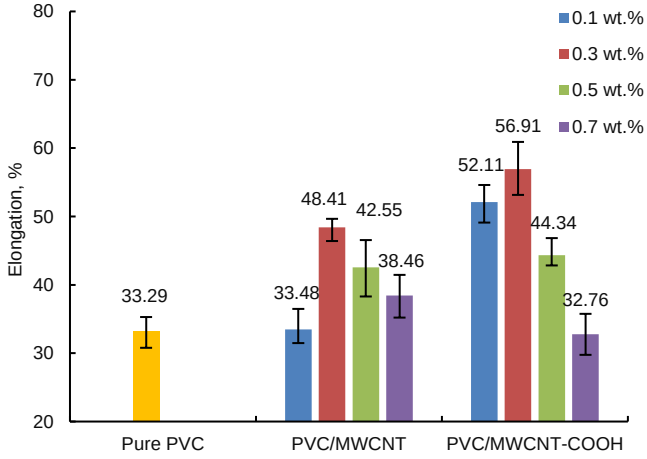

Fig. 4. Elongation values for prepared membranes.

3.2. Mechanical properties

The tensile strength and elongation at the break of the membranes are shown in Figures 3 and 4. The modified PVC/MWCNT and PVC/MWCNT-COOH nanocomposite membranes showed higher tensile strength in comparison with the neat PVC membrane. The tensile strength increased from 4.3 MPa to 6.1 MPa for PVC/MWCNT 0.3 wt. % and 6.3 MPa for PVC/MWCNT-COOH 0.3 wt. % membranes, respectively. This increase in tensile strength could be attributed to the excellent mechanical properties of MWCNT such as its high aspect ratio, high surface area and inclusion as MWCNT are considered to be one of the stiffest and strongest materials [36]. In addition, interface interaction existed between the MWCNT-COOH and PVC substrate, which greatly improved the compatibility between the CNT and polymeric matrix so that the tensile strengths of modified membranes were improved remarkably when compared to the pure PVC membrane and the PVC/MWCNT membranes [37]. On the other hand, with the further increasing of MWCNT and MWCNT-COOH, the tensile strength and elongation slightly decreased; this may be due to the agglomeration that occurred as a result of increased MWCNT concentration and hence, accelerated the break of the membrane. Also, elongation at break for the modified PVC membranes increased with the increasing of the MWCNT and MWCNT-COOH concentration from 33.2 % for pristine PVC to 48.4 % for PVC/MWCNT 0.3 wt. % and 56.9 % for PVC/MWCNT-COOH, which was likely due to the suitability between the PVC and nanofillers. However, the reduction of the elongation by increasing nanofillers by more than 0.3 wt. % could be explained by the high rigidity of the membranes and as a result of the development of large finger-like pores and cavities.

3.3. Abrasion test

The polymeric membranes used in water treatment are mostly subjected to abrasion by solid particles. One of the necessary tests to evaluate them is the abrasion test. Fig. 5 represents the weight loss per unit area of pure PVC and all fabricated nanocomposite membranes after the abrasion test. It shows that in the presence of MWCNT-COOH, the lowest weight loss occurs. In the presence of raw MWCNT as the nanofiller, the weight loss is still lower than the pure PVC membrane. Interestingly, the PVC/MWCNT-COOH membrane shows superior performance and lower weight loss than the PVC/MWCNT membrane. This finding is mainly due to the existence of carboxyl groups on the surface of MWCNT-COOH, which enhances the MWCNT distribution as well as the contact reinforcement/matrix effect in the PVC matrix. This also indicates that the addition of MWCNT and MWCNT-COOH to the PVC membrane resulted in more abrasion-resistant membranes in comparison with pure PVC membrane. A similar result has been reported elsewhere [10,26].

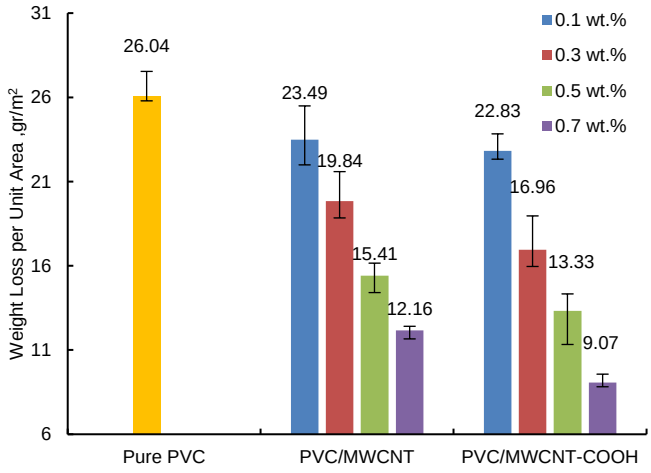

Fig. 5. Weight loss per unit area of the membranes after 7 days abrasion test with silicon carbide particles.

3.4. Morphology

FESEM imaging was utilized to investigate the changes in the cross-section and surface morphology of the nanocomposite membranes after the addition of pristine and modified MWCNT; the results are shown in Figure 6.The pore structure of the as-cast membranes was expected to be a function of a number of variables: viscosity during casting, the liquid-liquid demixing process driven by both affinity and miscibility, the polymer chain packing or free volume after deposition, and the state of agglomeration of nanoparticles [30,36,38-40]. As illustrated in Figure 6, the cross-section structures of all the membranes were asymmetric that consisted of three layers: a denser skin layer on the surface, a finger-like pore structure in the middle layer followed by a large macro void and/or sponge-like structure observed in the sub-layer. The denser skin layer on the surface seemed to have more and extended microvoids in both nanocomposite membranes in comparison with pure PVC membrane. The finger-like structure of both the composite membranes incorporated with MWCNT and MWCNT-COOH appeared to be extended and larger than that of a PVC membrane. It could be seen that the finger-like pore structure of the PVC/MWCNT-COOH nanocomposite membrane was narrower than the pure PVC and PVC/MWCNT nanocomposite membranes, which may be attributed to the higher solvent-non-solvent exchange rate created by hydrophilic MWCNT during the phase-inversion process and also the high affinity of MWCNT towards water [41,42]. By adding carboxylated MWCNT to the PVC matrix, the connectivity between microvoids, finger-like and macro voids was created across the membrane thickness [12]. The same results have been observed in PES/SiO_2 and PVC/Fe_2O_3 membranes [13]. Vatanpour et al. showed that by adding oxidized MWCNT up to 0.2 wt. %, the size of the top layers pores was enhanced, while a further increase in the oxidized MWCNT content caused a reduction in size [25]. Figure 6 also shows surface FESEM images of the membranes. As can be seen, all the membranes had a porous skin and the number of pores on the PVC/MWCNT-COOH membrane was higher than the neat PVC and PVC/MWCNT membranes. Moreover, the size of the pores on the PVC/MWCNT-COOH surface seemed smaller than that of the other membranes, and the results of the surface analyzing by ImageJ software (Figure 7) confirmed it. The statistical results from the image analyzer software revealed that the number of surface pores was 68, 1215 and 1220 for pure PVC, PVC/MWCNT and PVC/MWCNT-COOH, respectively, which indicated that the number of pores per unit area (pore density) increased at the presence of MWCNT. In membranes with more and smaller pores on the surface, water flux and rejection increase simultaneously; it will be shown that the performance of PVC/MWCNT-COOH membranes was higher than that of neat PVC and PVC/MWCNT membranes.

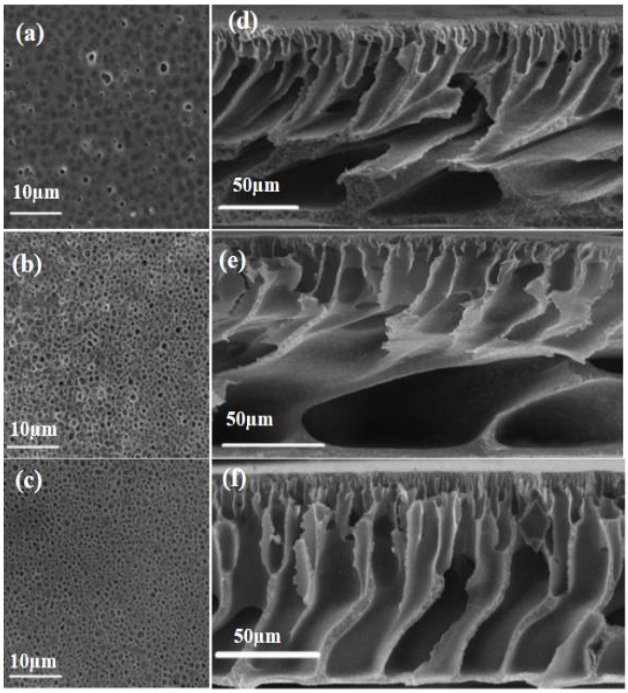

Fig. 6. Surface (left) and cross-section (right) FESEM of prepared membranes. (a) and (d) Pure PVC, (b) and (e) PVC/MWCNT 0.3 wt.%, (c) and (f) PVC/MWCNT-COOH 0.3 wt.%.

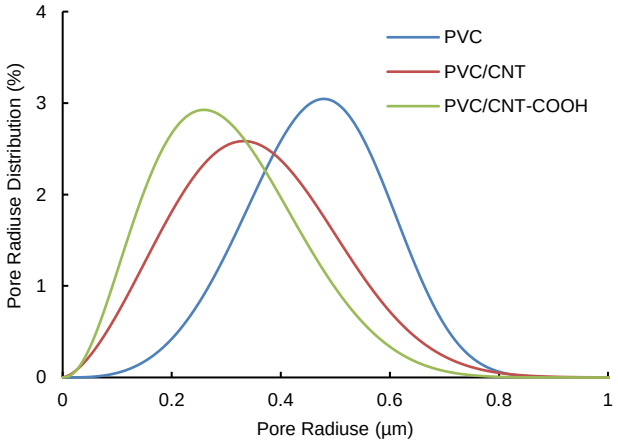

Fig.7. Pore size distribution of the prepared membranes.

3.5. Pure water flux

The pure water fluxes of the membranes are illustrated in Figure 8. Compared with the pure water flux of the pristine PVC membrane (244.8 L/ m^2h), the pure water flux of the PVC/MWCNT and PVC/MWCNT-COOH nanocomposite membranes were enhanced. When the content of the MWCNT and MWCNT-COOH increased to 0.3 wt. %, the water flux of PVC/MWCNT and PVC/MWCNT-COOH membranes reached a peak value of 484.7 L/m^2h and 526.2 L/m^2h, respectively. The flux improvement depended on membrane morphology and hydrophilicity. First, water flux had a direct relationship with the number of pores and the pore size on the membrane surface. As shown in Figures 6 and 7, the pores size of the nanocomposite membranes was smaller than those of pure PVC, but their numbers increased in very large amounts. Judging from Figure 6, the porosity of the PVC/carbon materials blend membranes was marginally higher than that of the pure PVC membrane. In addition, by embedding the nanofillers into the casting solution, the interaction between polymer chains and the nanofillers may disrupt the polymer chain packing, therefore improving water permeability due to the introduction of free volumes between the polymer chains and nanofiller interface [42]. Thus, these structural differences brought about the difference in the membranes water permeation flux. Second, as a rigid cylindrical nano-material, one-dimensional MWCNT with high specific area were regularly collocated in the PVC membrane and formed a nodular structure, so the surface of the membrane became rougher after the addition of MWCNT. During the phase inversion process, one-dimensional MWCNT easily migrated spontaneously to the membrane/water interface to reduce the interface energy and increase the surface hydrophilicity of membranes; consequently, this led to a further increase in the pure water flux of the nanocomposite membranes [29,31,43]. The PVC/MWCNT-COOH nanocomposite membranes indicated a higher pure water flux than the PVC/MWCNT which could be explained by their higher surface hydrophilicity. It can also be noted that by increasing the content of the nanofillers to more than 0.3 wt.% for both types of nanocomposite membranes, the pure water flux decreased. This was possibly due to the aggregation and low MWCNT dispersion in the PVC matrix, which led to less hydrophilicity and more blocked pores in the membrane.

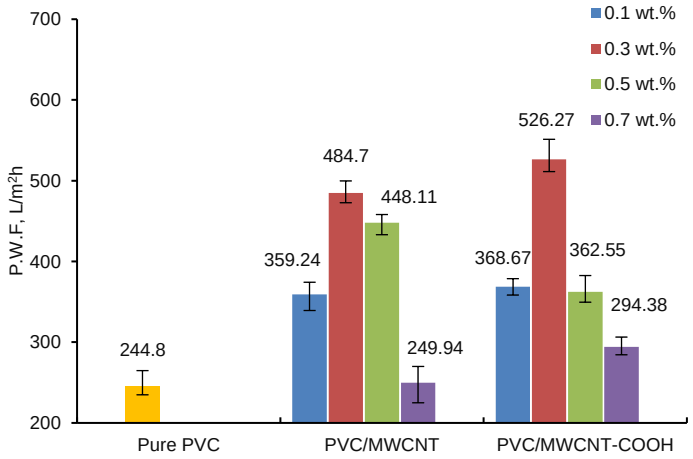

Fig. 8. Pure water flux of the prepared membranes.

3.6. Rejection

The ability of the all prepared membranes to reject humic acid was studied and the data are shown in Figure 9. The rejection of membranes was evaluated by measuring the concentration of HA in the feed and permeate stream. All the nanocomposite membranes showed a higher rejection of HA compared with pure PVC. The rejection of HA increased from 62.4 % for pure PVC to 96.0 % for PVC/MWCNT 0.7 wt. % and 96.8 % for PVC/MWCNT-COOH 0.7 wt. % nanocomposite membranes. The HA removal mechanism depends on two factors; the first is the average pore size of the membrane and the second is the adsorption of HA on the membrane surface [44]. By adding nanoparticles and when the concentrations of nanofillers increased to 0.7 wt%, the high density of MWCNT and MWCNT-COOH in the casting solution led to an increase in the viscosity of the solution. This prevented the exchange between the solvent and non-solvent during the phase separation process and slowed down the precipitation of the membrane; consequently, a relative smaller porous membrane was formed [37]. As shown previously, the mean pore radius of nanocomposite membranes decreased as the content of nanofillers increased. Decreasing the mean pore radius of membranes led to a drawback of more HA molecules, which consequently resulted in higher rejection. The smaller the pores, the higher the rejection. In addition, an increase in rejection could be explained by the fact the HA molecules were adsorbed on the MWCNT and rejected from the permeate solution [30,45]. The presence of embedded nanoparticles may also contribute to the degradation of HA molecules and enhance HA removal [33].

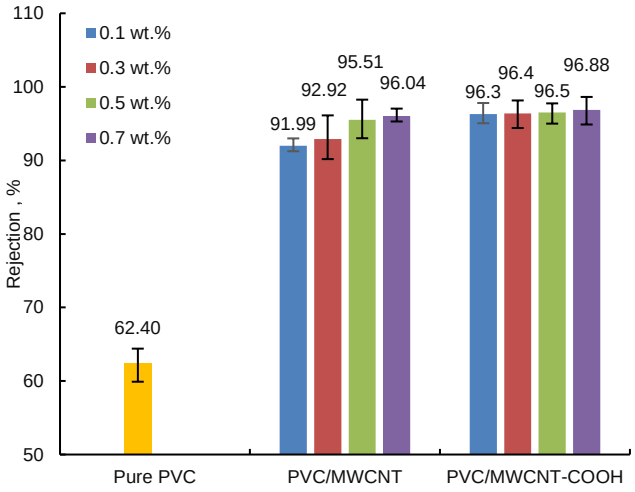

Fig. 9. HA rejection of all prepared membranes.

3.7. Antifouling properties

The flux-time curves for the prepared membranes during filtration of a 0.1 g/L HA solution are illustrated in Figures 10 and 11. The results in Figures. 10 and 11 reveal that the flux of the neat PVC membrane was the least among the membranes, and its value decreased from 95 L/m^{2}h to about 25 L/m^{2}h after 240 min. On the other hand, in comparison with pure PVC, the incorporation of both nanofillers increased the flux. The HA solution flux for the PVC/MWCNT-COOH (0.3 wt %) nanocomposite membrane was higher than other membranes. This result indicated that the membrane hydrophilicity played a vital role in the improvement of HA solution flux and the antifouling properties of the membranes increased with increasing hydrophilicity [10,34,46]. In addition, these results may be related to the surface pore sizes of the membranes. It has been proven that the membranes with larger pore size at the surface fouled easily and as shown before, the pore sizes of the membranes shifted towards smaller pores by the addition of MWCNT and MWCNT-COOH [47].

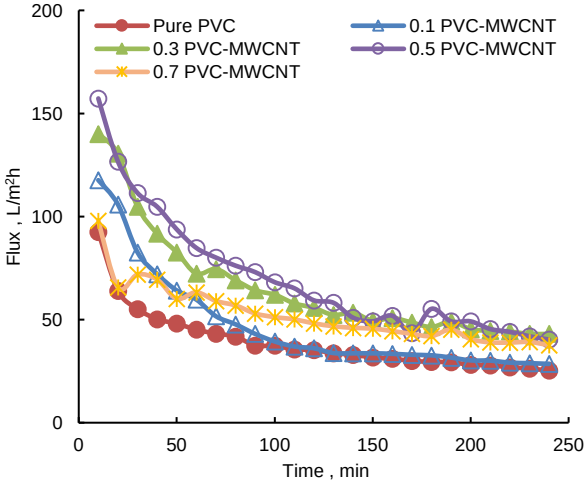

Fig. 10. Flux-time behavior of pure PVC and PVC/MWCNT membranes in the filtration process of HA solution.

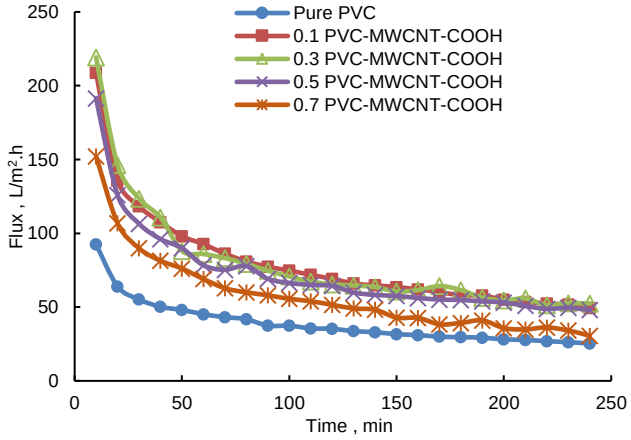

Fig. 11. Flux-time behavior of pure PVC and PVC/MWCNT-COOH membranes in the filtration process of HA solution.

The fouling analysis was carried out by calculating the reversible fouling ratio (RFR), irreversible fouling ratio (IFR), total fouling ratio (TFR), and flux recovery ratio (FRR) of the membranes which were defined in section 2.4.7. These parameters were estimated based on the pure water flux and filtration flux of the HA solution; the results are summarized in Figures 12 and 13. The results showed that the TFR of the membranes decreased from 61.4% for the pure PVC membrane to 35.4% for the PVC/MWCNT 0.5 wt. % and 35.8 for the PVC/MWCNT-COOH nanocomposite membranes; it then increased for membranes with higher contents of nanofillers, but almost all the nanocomposite membranes had a lower TFR than the pure PVC membrane. The lower values of TFR showed that less HA adsorption took place on the membrane surface or pore walls and referred to better antifouling properties. Also, it could be seen that by the addition of both nanofillers, the RFR of all nanocomposite membranes increased, which meant that most of the fouling of nanocomposite membranes could be cleaned easily by conventional cleaning methods. The IRF of all nanocomposite membranes were less than the pure PVC membrane and it reached its lowest amount of PVC/MWCNT-COOH nanocomposite membranes. As the membrane surface became more hydrophilic, the membrane's fouling was reduced; therefore, the higher hydrophilicity and subsequently higher FRR of the PVC/MWCNT-COOH (0.3 wt %) membranes created a lower fouling tendency than those of the PVC and PVC/MWCNT (0.3 wt %) membranes. Therefore, the results indicated that the PVC/MWCNT-COOH 0.3 wt.% membrane was more fouling resistant than the pure PVC membrane, and this membrane had the lowest fouling during 4 h of filtration of the HA solution [10,11].

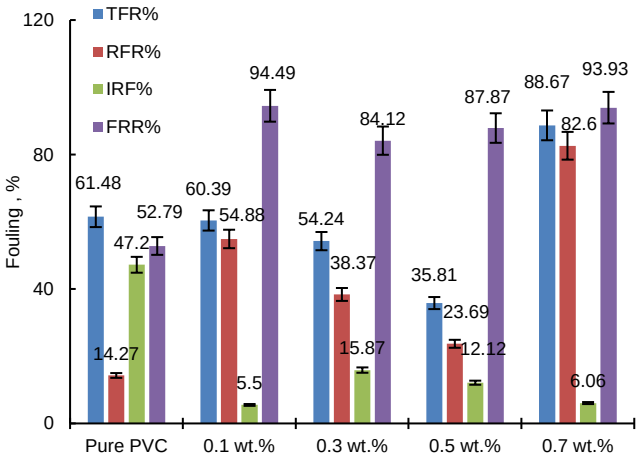

Fig. 12. Fouling parameters of pure PVC and PVC/MWCNT membranes.

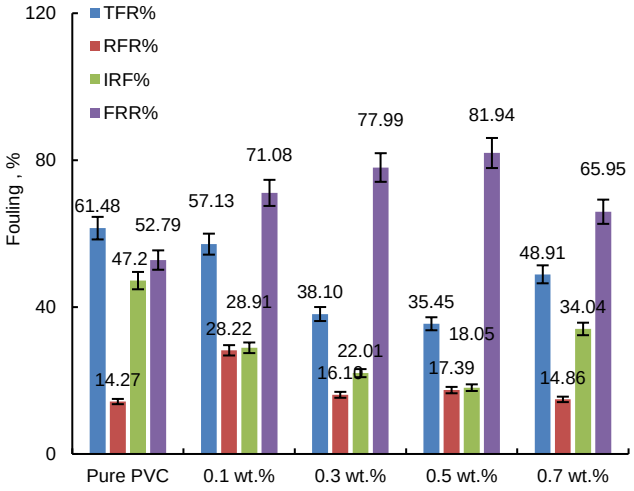

Fig. 13. Fouling parameters of pure PVC and PVC/MWCNT-COOH membranes.

4. Conclusions

The functionalized multi-walled carbon nanotubes (MWCNT-COOH) embedded polyvinyl chloride (PVC) membranes were prepared through solution casting by the phase inversion method. The functionalization of MWCNTwas performed for the purpose of better dispersion in organic solvents and improved compatibility with the polymeric matrix. The PVC/MWCNT and PVC/MWCNT-COOH nanocomposite membranes with different contents of nanofillers were prepared and characterized by a set of analyses. The results of FTIR revealed that a COOH group was formed on the surface of the MWCNT. The FESEM cross-section images indicated remarkable changes in the nanocomposite membrane structure and connectivity among finger-like pores and macro voids. The results of the surface FESEM images and pore size analyses showed that by the addition of both nano-fillers, the pores size of the membranes shifted to smaller pores and theirs numbers increased. This led to a higher pure water flux and a higher HA rejection for nanocomposite membranes. The obtained results revealed that the nanocomposite membranes fabricated by 0.3 wt. % MWCNT and MWCNT-COOH exposed the high hydrophilicity and excellent antifouling properties due to the increased hydrophilicity. The nanocomposite membranes also possessed higher tensile strength, higher abrasion resistance and higher elongation. In conclusion, the fabrication of the PVC/MWCNT and PVC/MWCNT-COOH nanocomposite membranes resulted in high-performance membranes with improved antifouling properties; the PVC/MWCNT-COOH 0.3 wt. % membrane was chosen as the best membrane in this study.

References

[1] Li, C., Cabassud, C., Guigui, C. (2015). Evaluation of membrane bioreactor on removal of pharmaceutical micropollutants: a review. *Desalination and water treatment*, *55*(4), 845-858.

[2] Maqbool, T., Khan, S. J., Lee, C. H. (2014). Effects of filtration modes on membrane fouling behavior and treatment in submerged membrane bioreactor. *Bioresource technology*, *172*, 391-395.

[3] Chakraborty, S., Drioli, E., Giorno, L. (2012). Development of a two separate phase submerged biocatalytic membrane reactor for the production of fatty acids and glycerol from residual vegetable oil streams. *Biomass and bioenergy*, *46*, 574-583.

[4] Tang, B., Yu, C., Bin, L., Zhao, Y., Feng, X., Huang, S., Chen, Q. (2016). Essential factors of an integrated moving bed biofilm reactor–membrane bioreactor: Adhesion characteristics and microbial community of the biofilm. *Bioresource technology*, *211*, 574-583.

[5] Ghaemi, N., Madaeni, S. S., Alizadeh, A., Daraei, P., Vatanpour, V., Falsafi, M. (2012). Fabrication of cellulose acetate/sodium dodecyl sulfate nanofiltration membrane: characterization and performance in rejection of pesticides. *Desalination*, *290*, 99-106.

[6] Ng, L. Y., Mohammad, A. W., Leo, C. P., Hilal, N. (2013). Polymeric membranes incorporated with metal/metal oxide nanoparticles: a comprehensive review. *Desalination*, *308*, 15-33.

[7] Xu, J., & Xu, Z. L. (2002). Poly (vinyl chloride)(PVC) hollow fiber ultrafiltration membranes prepared from PVC/additives/solvent. *Journal of membrane science*, *208*(1-2), 203-212.

[8] Zhang, X., Chen, Y., Konsowa, A. H., Zhu, X., Crittenden, J. C. (2009). Evaluation of an innovative polyvinyl chloride (PVC) ultrafiltration membrane for wastewater treatment. *Separation and purification technology*, *70*(1), 71-78.

[9] Jafarzadeh, Y., Yegani, R., Sedaghat, M. (2015). Preparation, characterization and fouling analysis of ZnO/polyethylene hybrid membranes for collagen

separation. *Chemical engineering research and design*, *94*, 417-427.

[10] Behboudi, A., Jafarzadeh, Y., Yegani, R. (2017). Polyvinyl chloride/polycarbonate blend ultrafiltration membranes for water treatment. *Journal of membrane science*, *534*, 18-24.

[11] Behboudi, A., Jafarzadeh, Y., Yegani, R. (2016). Preparation and characterization of TiO2 embedded PVC ultrafiltration membranes. *Chemical engineering research and design*, *114*, 96-107.

[12] Rabiee, H., Vatanpour, V., Farahani, M. H. D. A., Zarrabi, H. (2015). Improvement in flux and antifouling properties of PVC ultrafiltration membranes by incorporation of zinc oxide (ZnO) nanoparticles. *Separation and purification technology*, *156*, 299-310.

[13] Demirel, E., Zhang, B., Papakyriakou, M., Xia, S., Chen, Y. (2017). Fe_2O_3 nanocomposite PVC membrane with enhanced properties and separation performance. *Journal of membrane science*, *529*, 170-184.

[14] Yin, J., Zhu, G., Deng, B. (2013). Multi-walled carbon nanotubes (MWNTs)/polysulfone (PSU) mixed matrix hollow fiber membranes for enhanced water treatment. *Journal of membrane science*, *437*, 237-248.

[15] Byrne, M. T., Gun'ko, Y. K. (2010). Recent advances in research on carbon nanotube–polymer composites. *Advanced materials*, *22*(15), 1672-1688.

[16] Gaur, M. S., Singh, R., Tiwari, R. K. (2014). Study of structural morphology, thermal degradation and surface charge decay in PU+ PSF+ CNTs polymer hybrid nanocomposite. *Journal of electrostatics*, *72*(4), 242-251.

[17] Pekker, S., Salvetat, J. P., Jakab, E., Bonard, J. M., Forro, L. (2001). Hydrogenation of carbon nanotubes and graphite in liquid ammonia. *The journal of physical chemistry B*, *105*(33), 7938-7943.

[18] Holzinger, M., Vostrowsky, O., Hirsch, A., Hennrich, F., Kappes, M., Weiss, R., Jellen, F. (2001). Sidewall functionalization of carbon nanotubes. *Angewandte chemie international edition*, *40*(21), 4002-4005.

[19] Mickelson, E. T., Huffman, C. B., Rinzler, A. G., Smalley, R. E., Hauge, R. H., Margrave, J. L. (1998). Fluorination of single-wall carbon nanotubes. *Chemical physics letters*, *296*(1-2), 188-194.

[20] Georgakilas, V., Kordatos, K., Prato, M., Guldi, D. M., Holzinger, M., Hirsch, A. (2002). Organic functionalization of carbon nanotubes. *Journal of the American chemical society*, *124*(5), 760-761

[21] Ying, Y., Saini, R. K., Liang, F., Sadana, A. K., Billups, W. E. (2003). Functionalization of carbon nanotubes by free radicals. *Organic letters*, *5*(9), 1471-1473.

[22] Bahr, J. L., Yang, J., Kosynkin, D. V., Bronikowski, M. J., Smalley, R. E., Tour, J. M. (2001). Functionalization of carbon nanotubes by electrochemical reduction of aryl diazonium salts: a bucky paper electrode. *Journal of the American chemical society*, *123*(27), 6536-6542.

[23] Suhartono, J., Tizaoui, C. (2015). Polyvinylidene fluoride membranes impregnated at optimised content of pristine and functionalised multi-walled carbon nanotubes for improved water permeation, solute rejection and mechanical properties. *Separation and purification technology*, *154*, 290-300.

[24] Daraei, P., Madaeni, S. S., Ghaemi, N., Monfared, H. A., Khadivi, M. A. (2013). Fabrication of PES nanofiltration membrane by simultaneous use of multi-walled carbon nanotube and surface graft polymerization method: comparison of MWCNT and PAA modified MWCNT. *Separation and purification technology*, *104*, 32-44.

[25] Vatanpour, V., Madaeni, S. S., Moradian, R., Zinadini, S., Astinchap, B. (2011). Fabrication and characterization of novel antifouling nanofiltration membrane prepared from oxidized multiwalled carbon nanotube/polyethersulfone nanocomposite. *Journal of membrane science*, *375*(1-2), 284-294.

[26] Lai, C. Y., Groth, A., Gray, S., Duke, M. (2014). Enhanced abrasion resistant PVDF/nanoclay hollow fibre composite membranes for water treatment. *Journal of membrane science*, *449*, 146-157.

[27] Safarpour, M., Khataee, A., Vatanpour, V. (2015). Effect of reduced graphene oxide/TiO_2 nanocomposite with different molar ratios on the performance of PVDF ultrafiltration membranes. *Separation and purification technology*, *140*, 32-42.

[28] Palacio, L., Calvo, J. I., Prádanos, P., Hernández, A., Väisänen, P., Nyström, M. (1999). Contact angles and external protein adsorption onto UF membranes. *Journal of membrane science*, *152*(2), 189-201.

[29] Zhao, Y., Xu, Z., Shan, M., Min, C., Zhou, B., Li, Y., Qian, X. (2013). Effect of graphite oxide and multi-walled carbon nanotubes on the microstructure and performance of PVDF membranes. *Separation and purification technology*, *103*, 78-83.

[30] Esfahani, M. R., Tyler, J. L., Stretz, H. A., Wells, M. J. (2015). Effects of a dual nanofiller, nano-TiO_2 and MWCNT, for polysulfone-based nanocomposite membranes for water purification. *Desalination*, *372*, 47-56.

[31] Celik, E., Park, H., Choi, H., Choi, H. (2011). Carbon nanotube blended polyethersulfone membranes for fouling control in water treatment. *Water research*, *45*(1), 274-282.

[32] Celik, E., Liu, L., Choi, H. (2011). Protein fouling behavior of carbon nanotube/polyethersulfone composite membranes during water filtration. *water research*, *45*(16), 5287-5294.

[33] Jung, G., Kim, H. I. (2014). Synthesis and photocatalytic performance of PVA/TiO_2/graphene-MWCNT

nanocomposites for dye removal. *Journal of applied polymer science*, *131*(17), doi.org/10.1002/app.40715.

[34] Etemadi, H., Yegani, R., Babaeipour, V. (2017). Performance evaluation and antifouling analyses of cellulose acetate/nanodiamond nanocomposite membranes in water treatment. *Journal of applied polymer science*, *134*(21), doi.org/10.1002/app.44873.

[35] Yuliwati, E., Ismail, A. F. (2011). Effect of additives concentration on the surface properties and performance of PVDF ultrafiltration membranes for refinery produced wastewater treatment. *Desalination*, *273*(1), 226-234.

[36] Yang, Y. N., Jun, W., Qing-zhu, Z., Xue-si, C., Hui-xuan, Z. (2008). The research of rheology and thermodynamics of organic–inorganic hybrid membrane during the membrane formation. *Journal of membrane science*, *311*(1-2), 200-207.

[37] Khan, R., Khare, P., Baruah, B. P., Hazarika, A. K., Dey, N. C. (2011). Spectroscopic, kinetic studies of polyaniline-flyash composite. *Advances in chemical engineering and sciences*, *1*, 37-44.

[38] Zhao, W., Su, Y., Li, C., Shi, Q., Ning, X., Jiang, Z. (2008). Fabrication of antifouling polyethersulfone ultrafiltration membranes using Pluronic F127 as both surface modifier and pore-forming agent. *Journal of membrane science*, *318*(1-2), 405-412.

[39] Kimmerle, K., Strathmann, H. (1990). Analysis of the structure-determining process of phase inversion membranes. *Desalination*, *79*(2-3), 283-302.

[40] Fontananova, E., Jansen, J. C., Cristiano, A., Curcio, E., Drioli, E. (2006). Effect of additives in the casting solution on the formation of PVDF membranes. *Desalination*, *192*(1-3), 190-197.

[41] Arsuaga, J. M., Sotto, A., Del Rosario, G., Martínez, A., Molina, S., Teli, S. B., de Abajo, J. (2013). Influence of the type, size, and distribution of metal oxide particles on the properties of nanocomposite ultrafiltration membranes. *Journal of membrane science*, *428*, 131-141.

[42] Wang, W. Y., Shi, J. Y., Wang, J. L., Li, Y. L., Gao, N. N., Liu, Z. X., Lian, W. T. (2015). Preparation and characterization of PEG-g-MWCNTs/PSf nano-hybrid membranes with hydrophilicity and antifouling properties. *RSC Advances*, *5*(103), 84746-84753.

[43] Sun, M., Su, Y., Mu, C., Jiang, Z. (2009). Improved antifouling property of PES ultrafiltration membranes using additive of silica− PVP nanocomposite. *Industrial and engineering chemistry research*, *49*(2), 790-796.

[44] Amy, G. L. (2001). *NOM rejection by, and fouling of, NF and UF membranes*. American water works association.

[45] Heo, J., Kim, H., Her, N., Lee, S., Park, Y. G., Yoon, Y. (2012). Natural organic matter removal in single-walled carbon nanotubes–ultrafiltration membrane systems. *Desalination*, *298*, 75-84.

[46] Akbari, A., Yegani, R., Pourabbas, B., Behboudi, A. (2016). Fabrication and study of fouling characteristics of HDPE/PEG grafted silica nanoparticles composite membrane for filtration of Humic acid. *Chemical engineering research and design*, *109*, 282-296.

[47] Fu, X., Maruyama, T., Sotani, T., Matsuyama, H. (2008). Effect of surface morphology on membrane fouling by humic acid with the use of cellulose acetate butyrate hollow fiber membranes. *Journal of membrane science*, *320*(1-2), 483-491.